Molecular Biology of the Cell
Vol. 12, 3668–3679, November 2001

In Vivo Role for Actin-regulating Kinases in Endocytosis and Yeast Epsin Phosphorylation

Hadiya A. Watson,* M. Jamie T. V. Cope,† Aaron Chris Groen,† David G. Drubin,† and Beverly Wendland*‡

*Department of Biology, The Johns Hopkins University, Baltimore, Maryland 21218; and † Molecular and Cell Biology, The University of California, Berkeley, California 94720-3202

Submitted March 21, 2001; Revised August 7, 2001; Accepted August 16, 2001
Monitoring Editor: Tim Stearns

The yeast actin-regulating kinases Ark1p and Prk1p are signaling proteins localized to cortical actin patches, which may be sites of endocytosis. Interactions between the endocytic proteins Pan1p and End3p may be regulated by Prk1p-dependent threonine phosphorylation of Pan1p within the consensus sequence [L/I]xxQxTG. We identified two Prk1p phosphorylation sites within the Pan1p-binding protein Ent1p, a yeast epsin homologue, and demonstrate Prk1p-dependent phosphorylation of both threonines. Converting both threonines to either glutamate or alanine mimics constitutively phosphorylated or dephosphorylated Ent1p, respectively. Synthetic growth defects were observed in a *pan1–20 ENT1^{EE}* double mutant, suggesting that Ent1p phosphorylation negatively regulates the formation/activity of a Pan1p–Ent1p complex. Interestingly, *pan1–20 ent2*Δ but not *pan1–20 ent1*Δ double mutants had improved growth and endocytosis over the *pan1–20* mutant. We found that actin-regulating Ser/Thr kinase (ARK) mutants exhibit endocytic defects and that overexpressing either wild-type or alanine-substituted Ent1p partially suppressed phenotypes associated with loss of ARK kinases, including growth, endocytosis, and actin localization defects. Consistent with synthetic growth defects of *pan1–20 ENT1^{EE}* cells, overexpressing glutamate-substituted Ent1p was deleterious to ARK mutants. Surprisingly, overexpressing the related Ent2p protein could not suppress ARK kinase mutant phenotypes. These results suggest that Ent1p and Ent2p are not completely redundant and may perform opposing functions in endocytosis. These data support the model that, as for clathrin-dependent recycling of synaptic vesicles, yeast endocytic protein phosphorylation inhibits endocytic functions.

INTRODUCTION

Endocytosis is an essential process in eukaryotic cells during which portions of the plasma membrane and extracellular fluid are internalized, delivered to endosomes, and either recycled back to the plasma membrane or targeted to a degradation compartment. Clathrin-dependent receptor-mediated endocytosis remains the most well characterized endocytic mechanism to date (reviewed in Schmid, 1997). In this pathway, the cytosolic tail of a receptor associates with an adaptor complex that recruits and promotes the polymerization of clathrin triskelions into baskets, forming a clathrin-coated pit invagination. A fission event involving several proteins, including the GTPase dynamin, culminates in the release of a clathrin-coated vesicle into the cytosol.

The budding yeast *Saccharomyces cerevisiae* has been used as a model organism for identifying novel endocytic factors. We found that Pan1p is required for endocytosis and normal actin cytoskeleton organization in yeast (Wendland *et al.*, 1996; Wendland and Emr, 1998); others have identified and characterized *pan1* mutants in independent screens (Zoladek *et al.*, 1995; Tang and Cai, 1996). Pan1p has a domain organization similar to the mammalian endocytosis protein Eps15 (Wong *et al.*, 1995; Wendland *et al.*, 1996; Carbone *et al.*, 1997; Benmerah *et al.*, 2000), and both contain Eps15 homology (EH) domains that bind the tripeptide Asn-Pro-Phe (NPF) (de Beer *et al.*, 1998, 2000; Salcini *et al.*, 1999). The EH domains of Eps15 interact with epsin, an Asn-Pro-Phe-containing protein also required for endocytosis (Chen *et al.*, 1998). We recently identified the yeast epsin homologues Ent1p and Ent2p that interact in an analogous manner with the EH domains of Pan1p (Wendland *et al.*, 1999).

Epsin (Eps15 interactor) proteins comprise a novel family of interacting partners for components of the clathrin endocytic machinery (Chen, *et al.*, 1998; Rosenthal, *et al.*, 1999). Vertebrate epsins bind EH domain-containing proteins, AP-2, and clathrin. The NH_2-terminal 140 amino acids of epsins constitute a highly conserved module termed the

‡ Corresponding author. E-mail address: beverly@jhu.edu.
Abbreviations used: ARK, actin regulating kinase; EH, Eps15 homology; ENTH, epsin N-terminal homology; NPF, Asn-Pro-Phe; PIP_2, phosphatidylinositol 4,5 bisphosphate.

epsin–NH_2-terminal homology (ENTH) domain, which has recently been implicated in nuclear shuttling via an interaction with the transcription factor promyelocytic leukemia Zn^{2+} finger protein (Kay *et al.*, 1999; Hyman *et al.*, 2000) and can also bind the phospholipid phosphatidylinositol 4,5 bisphosphate (Itoh *et al.*, 2001). As with mammalian epsin, the Ent1p and Ent2p proteins contain ENTH domains, bind clathrin, and are required for endocytosis.

Phosphorylation as a means to control interactions between endocytic proteins has been proposed in mammalian systems (Slepnev *et al.*, 1998; Chen *et al.*, 1999). Both Eps15 and epsin are dephosphins, endocytic proteins that are phosphorylated in resting nerve terminals and coordinately dephosphorylated during stimulation (Chen *et al.*, 1998). It was shown recently that the yeast eps15-like protein, Pan1p, is phosphorylated in vitro by the novel Ser/Thr kinase, Prk1p, on regions containing the consensus sequence LxxQxTG, and it was proposed that Prk1p-dependent phosphorylation may negatively regulate the formation of an endocytic complex between Pan1p and End3p (Zeng and Cai, 1999). Prk1p, originally called Pak1p (Thiagalingam *et al.*, 1995), belongs to a novel family of ARKs composed of three proteins: Prk1p, Ark1p, and Akl1p (Cope *et al.*, 1999). Ark1p and Prk1p are localized to cortical actin patches in yeast. Although these patches may correspond to sites of endocytosis, the molecular links between actin organization and endocytosis remain undefined (Mulholland *et al.*, 1999; Qualmann *et al.*, 2000). Targets of the ARK kinases, such as Pan1p, are good candidates for factors that link endocytosis and actin organization. Here, we report that both Ent1p and Ent2p are also targets of Prk1p. Mutant forms of Ent1p that mimic constitutively phosphorylated or dephosphorylated states exhibit distinct genetic interactions with both *ark1*Δ *prk1*Δ and *pan1–20* mutants. The nature of these interactions suggest that, as in mammalian systems, dephosphorylated forms of yeast endocytic proteins promote internalization, whereas phosphorylation is inhibitory.

MATERIALS AND METHODS

Media and Materials

Yeast strains were grown in standard yeast extract–peptone–dextrose (YPD) or synthetic medium with dextrose supplemented with the appropriate amino acids as required for plasmid maintenance. Bacterial strains were grown on standard media supplemented with 100 μg/ml ampicillin or 30 μg/ml kanamycin, as appropriate, to maintain plasmids. Materials were purchased from Fisher Scientific (Fairlawn, NJ) or Sigma (St. Louis, MO) unless stated otherwise.

Plasmid Strain and Construction

The strains and plasmids used in this study are listed in Table 1. DNA and strain manipulations were performed with the use of standard techniques. All green fluorescent protein (GFP) tags used in this study are N terminal and are driven by the CPY promoter carboxypeptidase y, giving approximately equivalent protein expression levels to endogenous promoters.

FM 4–64 Internalization

Cells were grown to midlog phase in selective medium or YPD at 30°C. When appropriate, cells were shifted to 37°C for 45 min. One milliliter of cells was pelleted at 300 × *g* for 30 s and resuspended in 50 μl of prewarmed FM 4–64 dye diluted 1:100 in YPD (FM 4–64 stock is 1 mg/ml in dimethylsulfoxide). After 15–20 min labeling, the cells were washed, chased for 40–60 min, and observed. All images were acquired at identical exposures with the use of a Delta Vision deconvolving microscope (Applied Precision, Seattle, WA) with a cooled CCD camera and processed identically with the use of Adobe Photoshop 5.0. For quantification of FM 4–64 internalization, pixel intensities were measured from a single focal plane for ~35–50 cells from each strain.

Filamentous Actin and GFP-Ent1p and GFP-Ent2p Localization

Cells were grown to midlog phase at 30°C. $KHPO_4$ (1 M), pH 6.4 (2 KH_2P0_4:1 K_2HP0_4), and 37% formaldehyde were then added directly to each cell culture flask to a final concentration of 0.1 M and 4%, respectively, and cells were incubated with shaking for 1–2 h. After three washes in PBS, cells were permeabilized with 0.02% Triton X-100 for 10 min. Cells were labeled by resuspending in 30–50 μl of 0.6 μM rhodamine-phalloidin and 1 μM DAPI in PBS (Molecular Probes, Eugene, OR) for 2h. Cells were then washed, mounted in DABCO (triethylene-diamine) anti-fade solution (Sigma, St. Louis, MO), and observed with the use of a Delta Vision Deconvolving microscope.

For GFP/phalloidin double staining, cells expressing GFP constructs were grown to midlog phase in selective medium, harvested, then labeled and permeabilized concomitantly by incubating for 10 min at room temperature in the dark in a solution containing 0.3 μM rhodamine–phalloidin in 1 M Sorbitol, 0.1% Saponin, 0.1 mg/ml RNase, PBS, 5 mM $MgCl_2$, and 1 mM $CaCl_2$, followed by 15–20 min incubation on ice. The cells were viewed directly without washing.

Immunoprecipitation Experiments

Preparation of Yeast Cell Extracts. Five or 10 OD_{600} of cells grown to midlog phase were harvested, and cell pellets were precipitated in 10% TCA with protease/phosphatase inhibitors (250 mM NaF, 10 mM EDTA, 4 mM Na-orthovanadate, 0.2 mM cyclosporin, 2 mM AEBSF). TCA pellets were washed with cold acetone and lysed by vortexing with 0.4 mm acid-washed glass beads in 100 μl of boiling buffer (1 M Tris, 0.5 M EDTA, 10% SDS) with proteases/phosphatase inhibitors. Lysates were mixed with 1 ml of TBS-T/BSA (0.25 M NaCl, 10 mM Tris, 0.25% Tween, 1% BSA) with protease/phosphatase inhibitors and spun for 10 min at 4°C, and the supernatant was used for immunoprecipitation.

Ent1p and Ent2p Immunoprecipitation Experiments. Epitope-tagged Ent1p, $Ent1p^{AA}$-HA, and $Ent1p^{EE}$-HA were immunoprecipitated from extracts prepared as above with 0.4 μl/OD_{600} of mouse α-HA (Covance, Berkeley, CA) for 1 h at 4°C. After 1 h, 10 μl of protein G Sepharose beads (Sigma) per OD_{600} were added, and immunoprecipitates were incubated for an additional hour at 4°C.

Immunoprecipitation of endogenous Ent1p and Ent2p was performed with the use of 0.25–0.5 μl/OD_{600} of rabbit polyclonal antiserum (custom increased by Scantibodies, Ramona, CA) directed against amino acids 325–456 of a GST-Ent1p C-terminal fusion protein, followed by incubation with 10 μl/OD_{600} of protein A Sepharose beads (Sigma). Also used to immunoprecipitate endogenous or HA-tagged Ent1p and Ent2p was rabbit α-phosphothreonine (Zymed, San Francisco, CA) at 0.8 μl/OD_{600}. Beads were washed once with 1 ml TBS–Tween 20 + protease/phosphatase inhibitors, twice with TBS–Tween–urea + protease/phosphatase inhibitors, and once more with TBS + protease/phosphatase inhibitors. Excess liquid was removed from the beads with the use of a Hamilton syringe. The dried beads were resuspended in 10 μl/OD_{600} protein sample buffer, heated to 70–80°C for 10 min, and pelleted for 1 min, and the supernatant was used for SDS-PAGE and Western blot analysis.

Table 1. Genotypes of yeast strains and plasmid descriptions

Strain	Genotype	Source
BWY520	*MAT**a** leu2-3 ura3-52 his3-Δ200 trp1-Δ901 lys2-801 suc2-Δ9 ent1::LEU2 ent2::HIS3 pENT1.1HA-GFP.426*	Wendland *et al*., 1999
BWY1038	*MAT**a** leu2-3 ura3-52 his3-Δ200 trp1-Δ901 lys2-801 suc2-Δ9 ent1::LEU:ent1[T394A, T416A] ent2::HIS3*	This study
BWY1039	*MAT**a** leu2-3 ura3-52 his3-Δ200 trp1-Δ901 lys2-801 suc2-Δ9 ent1::LEU:ent1[T394E, T416E] ent2::HIS3*	This study
BWY1041	*MATa leu2-3 ura3-52 his3-Δ200 trp1-Δ901 lys2-801 suc2-Δ9 ent1::LEU2 pan1-20*	This study
BWY1053	*MATα leu2-3 ura3-52 his3-Δ200 trp1-Δ901 lys2-801 suc2-Δ9 ent1::LEU2 ent2::HIS3 pENT2-GFP.426*	This study
BWY1051	*MAT**a** leu2-3 ura3-52 his3-Δ200 trp1-Δ901 lys2-801 suc2-Δ9 ent1::LEU2 ent2::HIS3* p*ENT2[T479A, T499A]*	This study
BWY1055	*MAT**a** leu2-3 ura3-52 his3-Δ200 trp1-Δ901 lys2-801 suc2-Δ9 ent1::LEU2 ent2::HIS3 pENT1ΔCterm*	This study
BWY1098	*MATα leu2-3 ura3-52 his3-Δ200 trp1-Δ901 lys2-801 suc2-Δ9 pan1-20 ent2::HIS3*	This study
BWY1100	*MATα leu2-3 ura3-52 his3-Δ200 trp1-Δ901 lys2-801 suc2-Δ9 ent1::LEU2:ent1[T394A, T416A] pan1-20*	This study
BWY1103	*MAT**a** leu2-3 ura3-52 his3-Δ200 trp1-Δ901 lys2-801 suc2-Δ9 ent1::LEU2:ent1[T394A, T416A] ent2::HIS3 pan1-20*	This study
BWY1107	*MAT**a** leu2-3 ura3-52 his3-Δ200 trp1-Δ901 lys2-801 suc2-Δ9 ent1::LEU2:ent1[T394E, T416E] pan1-20*	This study
BWY1113	*MAT**a** leu2-3 ura3-52 his3-Δ200 trp1-Δ901 lys2-801 suc2-Δ9 ent1::LEU2:ent1[T394E, T416E] ent2::HIS3 pan1-20*	This study
BWY1252	*MATa leu2-3 ura3-52 his3-Δ200 trp1-Δ901 lys2-801 suc2-Δ9 pan1-20 ent1::LEU2*	This study
DDY130	*MAT**a** his3-Δ200 ura3-52 leu2-3, 112 lys2-801*	Drubin laboratory strain
DDY1407	*MAT**a** ark1::HIS3 his3-Δ200 ura3-52 leu2-3, 112 lys2-801 ade2-1*	Drubin laboratory strain
DDY1558	*MATα prk1::LEU2 his3-Δ200 ura3-52 leu2-3, 112 lys2-801*	Drubin laboratory strain
DDY1885	*MATα ark::HIS3 prk1::LEU2 his3-Δ200 ura3-52 leu2-3, 112 lys2-801*	Drubin laboratory strain
DDY2104	*MATa akl1::KANMX his3-Δ200 ura3-52 leu2-3, 112 lys2-801*	Drubin laboratory strain
DDY2103	*MATα ark::HIS3 prk1::LEU2 akl1::KANMX his3-Δ200 ura3-52 leu2-3, 112 lys2-801*	Drubin laboratory strain
HWY40	*MAT**a** leu2-3 ura3-52 his3-Δ200 trp1-Δ901 lys2-801 suc2-Δ9 ent1::HIS3 ent2::HIS3 pENT2.416*	Wendland *et al*., 1999
HWY41	*MAT**a** leu2-3 ura3-52 his3-Δ200 trp1-Δ901 lys2-801 suc2-Δ9 ent1::LEU2 ent2::HIS3 pENT1.416*	Wendland *et al*., 1999
SEY6210	*MAT**a** leu2-3 ura3-52 his3-Δ200 trp1-Δ901 lys2-801 suc2-Δ9*	Emr laboratory strain

Plasmid	Description	Source
pENT1.416	*ENT1* ORF plus 289nt 5′ UTR and 1001nt 3′ UTR in pRS416	Wendland *et al*., 1999
pENT1.426	*ENT1* ORF plus 289nt 5′ UTR and 1001nt 3′ UTR in pRS426	Wendland *et al*., 1999
pENT1.1HA-GFP.426	*Sal*I in frame upstream of start AUG; blunt *Sal*I fragment of *ENT1* in blunt *Eco*RI of pGOGFP.426	Wendland *et al*., 1999
pENT1-GFP.426	*Sal*I in frame upstream of start AUG; *Sal*I/*Ssp*I of *ENT1* in *Kpn*I(blunt)/*Sal*I of pGOGFP.426	This study
pENT2-GFP.426	*Sal*I in frame upstream of start AUG; *Sal*I/*Hin*DII of *ENT2* in *Kpn*I(blunt)/*Sal*I of pGOGFP.426	This study
pENT1.317	*Hin*DIII fragment of *ENT1* in *Hin*DIII of pRS317	This study
pENT1.1HA.317	*Sac*I fragment (3′ end) of pENT1.1HA.414 into *Sac*I of pENT1.317	This study
pent1[T394A, T416A].416	Oligo/PCR-mediated mutation of pENT1.416	This study
pent1[T394A, T416A].426	*Bst*EII fragment of $ENT1^{AA}$ replacing *Bst*EII fragment of pENT1.426	This study
pent1[T394E, T416E].416	Oligo/PCR-mediated mutation of pENT1.416	This study
pent1[T394E, T416E].426	*Bst*EII fragment of $ENT1^{EE}$ replacing *Bst*EII fragment of pENT1.426	This study
pent1[T394A, T416A].1HA.317	*Bst*EII fragment of $ENT1^{AA}$ replacing *Bst*EII fragment of pENT1.1HA.317	This study
pent1[T394E, T416E].1HA.317	*Bst*EII fragment of $ENT1^{EE}$ replacing *Bst*EII fragment of pENT1.1HA.317	This study
pent1ΔC-term.414	drop out SpeI fragment from pENT1.414, blunt, self-ligate	This study
pDD556	*PRK1* ORF plus 385nt 5′ UTR and 284nt 3′ UTR in pRS316	Cope *et al*., 1999
pGOGFP.426	CPY promoter driving GFP (S65T) in pRS426	Cowles *et al*., 1997

Phosphatase Treatment

Five OD_{600} of cells were harvested and lysed as described above. To test for phosphate modifications of Ent1p, Ent1p-HA was immunoprecipitated as described above. Beads were washed in TBS-T buffer lacking phosphatase inhibitors, resuspended in phosphatase buffer (0.01 M Tris, 0.01 M $MgCl_2$, 1 M NaCl, 1 mM DTT, 0.1 mM AEBSF), and incubated with or without 1 μl of Lambda Protein Phosphatase (New England Biolabs, Beverly, MA). Two microliters of phosphatase inhibitors (see above) were added to appropriate control tubes, and samples were incubated at 30°C for 30 min. After 30 min,

samples were mixed with protein sample buffer and prepared for SDS-PAGE. To test for Prk1p-dependent mobility shifts of endogenous Ent1p and Ent2p, 0.4 OD_{600} of cell extract were incubated with or without 2 μl of calf intestinal alkaline phosphatase (New England Biolabs) in phosphatase buffer at 30°C for 30 min.

SDS-PAGE and Immunoblotting

Samples were separated on either 7.5 or 9% polyacrylamide mini gels at 30 mA constant current in SDS-PAGE running buffer (3 mM SDS, 25 mM Tris, 192 mM glycine) and transferred onto nitrocellulose membrane in transfer buffer (1 mM SDS, 48 mM Tris, 400 mM glycine, 10% methanol) at 80 V for 90 min. Blots were blocked for 1 h in 5% nonfat dried milk in Western wash buffer (0.25 M NaCl, 10 mM Tris, 0.025% Tween, pH 7.5) and incubated with the appropriate primary antibody for 1 h at room temperature (or overnight at 4°C) and with secondary antibody for 45 min to 1 h at room temperature.

Antibodies Used for Immunodetection

The following antibodies were used for immunodetection: mouse α-HA at 1:1000 for detection of Ent1p-HA; rabbit α-Ent1/2p at 1:20,000 for detection of endogenous Ent1p and Ent2p; rabbit α-phosphothreonine at 1:250 for detection of phosphothreonine modification; and rabbit α-phosphorylated amino acids (Zymed) at 1:1000 for detection of all phosphorylated amino acids on immunoprecipitated Ent1p-HA. Either goat α-rabbit or goat α-mouse–horseradish peroxidase (Pierce, Rockford, IL) at 1:5000 for 1 h at room temperature was used as secondary antibody for all blots. All antibody dilutions were in 5% milk in Western wash buffer, and the Pierce Supersignal Chemiluminescence detection system was used for visualization.

RESULTS

Ent1p Is Phosphorylated on Threonine Residues

A search of the proteins predicted by the *S. cerevisiae* Genome Database revealed that Ent1p and Ent2p each contain two candidate Prk1p consensus phosphorylation sites (L/IxxQxTG) and are thus possible targets of Prk1p. To determine whether Ent1p is a phosphoprotein, an HA-epitope–tagged Ent1p (Ent1p-HA) was immunoprecipitated from wild-type cell extracts, treated with lambda protein phosphatase in the presence (+) or absence (−) of phosphatase inhibitors, and analyzed by Western blotting (Figure 1A). No signal was detected from cells containing a plasmid encoding untagged Ent1p (Figure 1A, lanes 1, 6). In untreated immunoprecipitates, Ent1p-HA migrates as a broad series of ~66–75 kDa bands. These bands collapse into a single ~66 kDa band after phosphatase treatment (Figure 1A, lanes 2, 3), slightly higher than the predicted molecular weight of ~56 kDa, suggesting that the slower mobility species arose because of phosphorylation. Some of the phosphorylation occurred on threonine residues, because Ent1p-HA immunoprecipitates also reacted with an α-phosphothreonine antiserum (Figure 1A, lane 7). As expected, no phosphothreonine was detected in phosphatase-treated Ent1p-HA immunoprecipitates (Figure 1A, lane 8). Thus, Ent1p-HA is a phosphoprotein that contains phosphothreonine.

Ent1p Is Phosphorylated within Prk1p Consensus Sites on Thr Residues 394 and 416

We next asked whether the target Thr residues within the Prk1p consensus sites in Ent1p were subject to phosphorylation. HA-tagged Ent1p point mutants in which the two putative target Thr residues were converted to either Glu (T394E, T416E; EE) or Ala (T394A, T416A; AA) were expressed in wild-type cells. Wild-type or mutant forms (EE or AA) of Ent1p-HA were immunoprecipitated and analyzed by immunoblotting as described above (Figure 1B). The Ent1p point mutant proteins were stable but migrated more rapidly than wild-type Ent1p-HA (Figure 1B, lanes 1–3). Rabbit α-phosphothreonine antibodies failed to detect significant levels of phosphothreonine in the Ent1p-HA point mutants (Figure 1B, lanes 5, 6) as compared with wild-type Ent1p-HA (Figure 1B, lane 4). These data suggest that threonine phosphorylation of Ent1p is primarily on the two threonine residues within the putative Prk1p kinase target sites. Probing with an antiserum recognizing all phosphorylated amino acids (α-phosphoamino acids) showed residual phosphorylation in the point mutants, suggesting the presence of other phosphorylated residues within Ent1p (our unpublished results; and see below). In contrast, analogous threonine point mutant forms of Ent2p exhibited residual phosphothreonine modification, suggesting the presence of additional target threonines in this protein.

To examine phosphate modifications of native Ent1p and Ent2p, a rabbit polyclonal antiserum was produced against a region conserved between Ent1p and Ent2p (amino acids 325–456 of Ent1p). The specificity of this antiserum is demonstrated in Figure 1C. Whole-cell extracts of wild-type cells (lane 1), cells expressing only Ent1p (*ent2*Δ, lane 2), only Ent2p (*ent1*Δ, lane 3), or *ent1*Δ *ent2*Δ cells expressing an Ent1p construct lacking the C-terminal region used to generate the α-Ent1p/2p antiserum (denoted −, lane 4) were analyzed by immunoblotting with the α-Ent1/2p serum. Ent1p and Ent2p migrated as ~49 and 82 kDa doublet bands, respectively. The observed mobility of Ent1p is consistent with its predicted value of ~53 kDa, whereas Ent2p mobility is slightly slower than the predicted value of ~72 kDa. When rabbit α-phosphothreonine immunoprecipitates were probed with α-Ent1/2p serum, both endogenous yeast epsin proteins were detected (Figure 1C, lanes 5–7), consistent with phosphothreonine modifications on both native proteins. Two background bands that migrated below Ent1p and Ent2p were also detected on these immunoblots (Figure 1C, lane 8). The IgG heavy chain of rabbit α-phosphothreonine migrates just below Ent1p. The second nonspecific background band (marked with *) runs just below Ent2p. These data demonstrate that both Ent1p and Ent2p are phosphorylated on threonine residues.

Prk1p Is Required for Ent1p and Ent2p Phosphorylation

To determine whether Prk1p kinase is required for Ent1p and Ent2p phosphorylation, whole-cell extracts from five different ARK family deletion strains and wild-type cells were either mock treated (−) or treated (+) with phosphatase, and mobility shifts were examined by immunoblotting with rabbit α-Ent1/2p (Figure 1D). The slower mobility forms of endogenous Ent1p and Ent2p present in mock-treated wild-type cells collapsed into faster mobility bands during phosphatase treatment (Figure 1D, lanes 1, 2). Similar phosphatase-sensitive, slow-mobility bands were observed in extracts from *ark1*Δ cells (lane 3) but were absent in extracts from mock-treated *prk1*Δ and *ark1*Δ *prk1*Δ, and the

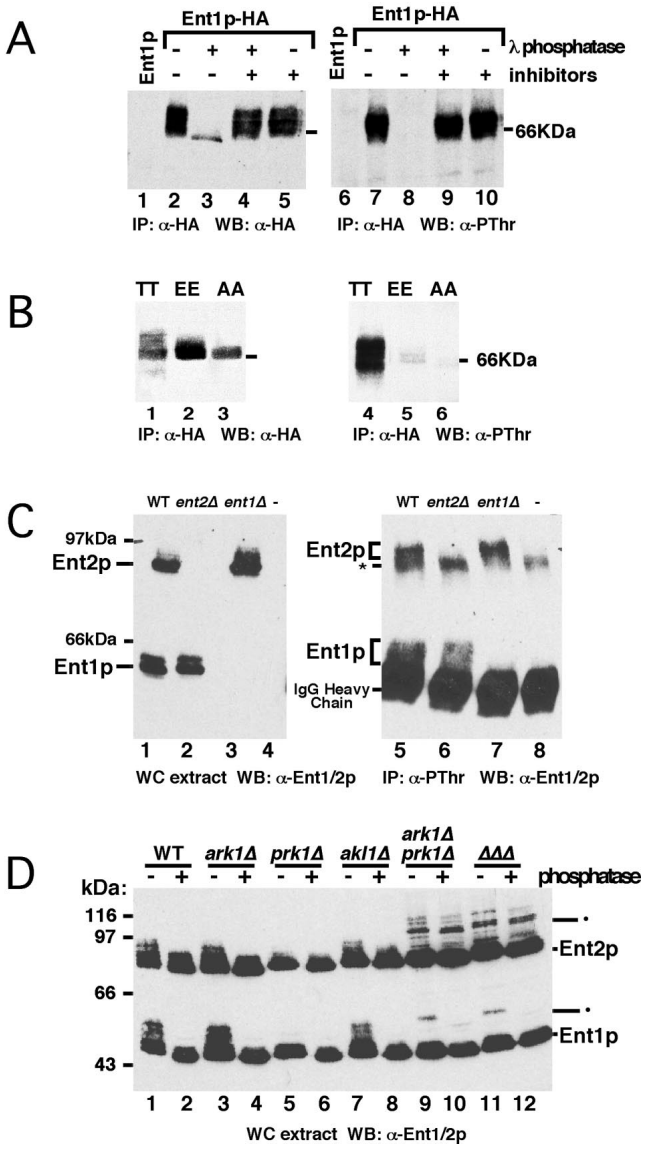

Figure 1. Ent1p and Ent2p threonine phosphorylation requires Prk1p. (A) Epitope-tagged Ent1p (Ent1p-HA) was immunoprecipitated, with the use of mouse α-HA, from wild-type cell extracts treated with lambda protein phosphatase and/or phosphatase inhibitors and analyzed on immunoblots. Left panel, rabbit α-HA; right panel, rabbit α-phosphothreonine. Lanes 1 and 6 correspond to immunoprecipitates from wild-type cells expressing untagged Ent1p; lanes 2–5 and 7–10 correspond to immunoprecipitates from wild-type cells expressing Ent1p-HA. (B) HA-tagged ent1p point mutants in which the two putative target Thr residues were converted to Ala (T394A, T416A; AA) or Glu (T394E, T416E; EE) were expressed in wild-type cells. Wild-type (TT) or mutant forms of Ent1p-HA were immunoprecipitated with the use of mouse α-HA and analyzed by immunoblotting. Left panel, rabbit α-HA; right panel, rabbit α-phosphothreonine. Lanes 1–3 and 4–6 each correspond to wild-type Ent1p-HA, Ent1p^{EE}-HA, and Ent1p^{AA}-HA immunoprecipitates, respectively. (C) Rabbit polyclonal antisera raised against a region of protein conserved between Ent1p and Ent2p (rabbit α-Ent1/2p) recognizes endogenous Ent1p and Ent2p in both whole-cell extracts (left panel) and rabbit α-phosphothreonine immunoprecipitates. Left panel, immunoblot of whole-cell extracts from wild-type cells (lane 1), *ent2*Δ cells (lane 2), *ent1*Δ cells (lane 3), and negative control *ent2*Δ cells expressing an Ent1p construct lacking the region used for generating rabbit α-Ent1/2p (lane 4). Right panel, endogenous Ent1p and Ent2p were immunoprecipitated from cells with the use of α-phosphothreonine and analyzed by immunoblotting with rabbit α-Ent1/2p. Nonspecific background bands are indicated by asterisk. (D) Whole-cell extracts from five different ARK family deletion strains and wild-type cells were either mock treated (−) or treated (+) with protein phosphatase and analyzed on immunoblots with the use of rabbit α-Ent1/2p. Phosphatase-resistant and/or slower mobility bands are indicated (•).

*ark1*Δ *prk1*Δ *akl1*Δ mutants (Figure 1D, lanes 5, 9, 11). These results suggest that Prk1p is required for Ent1p and Ent2p phosphorylation and are consistent with the inability of α-phosphothreonine to immunoprecipitate endogenous Ent1p and Ent2p from extracts of cells lacking *PRK1*. Also, although *akl1*Δ extracts contained phosphatase-sensitive, slow-mobility Ent1p and Ent2p (Figure 1D, lane 7), the intensity of these slower migrating species was consistently reduced as compared with wild-type and *ark1*Δ extracts, suggesting a possible role for Akl1p as an upstream activator of Prk1p. Similarly, reduced phosphothreonine levels were observed in Ent1p-HA immunoprecipitated from *akl1*Δ extracts.

Interestingly, even slower mobility forms of both Ent1p (~63 kDa) and Ent2p (~106 kDa) were observed exclusively in *ark1*Δ *prk1*Δ and *ark1*Δ *prk1*Δ *akl1*Δ extracts (Figure 1D, lanes 9–12, marked with •). Upper Ent2p bands were resistant to phosphatase treatment, whereas the upper Ent1p band was reduced in intensity and mobility in phosphatase-treated extracts. The significance of these upper bands remains to be determined.

*pan1–20 Interacts Genetically with ENT1^{EE} and ent2*Δ

Zeng and Cai (1999) showed previously that loss of Prk1p activity suppressed the temperature-sensitive growth of a pan1–4 mutant and that Prk1p phosphorylation may negatively regulate Pan1p/End3p interactions. These data suggest that Prk1p-mediated phosphorylation, possibly of a Pan1p complex, may serve an inhibitory function. In vivo genetic interactions between our *pan1–20* mutant and *ENT1^{AA}* and *ENT1^{EE}* point mutants as compared with wild-type *ENT1* were examined to test the hypothesis that Pan1p/Ent1p interactions may be phospho-regulated.

pan1 mutants exhibit defects in growth, endocytosis, and actin cytoskeleton organization at 37°C (Zoladek *et al.*, 1995; Tang and Cai, 1996; Wendland *et al.*, 1996; Tang *et al.*, 1997). To study genetic interactions between *pan1–20* and dephospho/phospho forms of Ent1p, we integrated *ENT1^{AA}* or *ENT1^{EE}* point mutant constructs into the *ent1* locus of *ent1*Δ *ent2*Δ cells (see MATERIALS AND METHODS). These *ENT1^{AA} ent2*Δ and *ENT1^{EE} ent2*Δ cells exhibited normal growth and actin cytoskeleton organization. Endocytosis of FM4–64 was normal in *ENT1^{AA} ent2*Δ cells, but the *ENT1^{EE} ent2*Δ mutant exhibited mild endocytic defects, suggesting that *ENT1^{EE}* is somewhat dominant; however, overexpressing *ENT1^{EE}* in wild-type cells did not appear to be dominant. Immunoblots of whole-cell extracts showed that although the levels of integrated Ent1p^{AA} are similar to wild-

Table 2. Summary of genetic interactions and phenotypes

Genotype	Actin organization	Endocytosis	Growth	Source
*ark1*Δ*prk1*Δ	Severely disrupted; actin clumps and depolarized patches	Reduced endocytic uptake; accumulation of endocytic intermediates	Slow at 30°C; poor on sorbitol at 30°C *ts* at 37°C	Cope *et al.*, 1999; and unpublished data
*ark1*Δ*prk1*Δ + *ENT1* 2μ	Similar to *ark1*Δ*prk1*Δ	Partial suppression of defective uptake	Suppression of *ts* and sorbitol-sensitive growth	This study
*ark1*Δ*prk1*Δ + $ENT1^{AA}$ 2μ[a]	Actin clumping is less severe than *ark1*Δ*prk1*Δ	Similar to *ark1*Δ*prk1*Δ + *ENT1* 2μ	Similar to *ark1*Δ*prk1*Δ + *ENT1* 2μ	This study
*ark1*Δ*prk1*Δ + $ENT1^{EE}$ 2μ[a]	Similar to *ark1*Δ*prk1*Δ	Endocytic defects enhanced	Similar to *ark1*Δ*prk1*Δ	This study
*ark1*Δ*prk1*Δ + *ENT2* 2μ[b]	Similar to *ark1*Δ*prk1*Δ	Similar to *ark1*Δ*prk1*Δ	Similar to *ark1*Δ*prk1*Δ	This study
pan1-20	Actin mislocalization and mild clumping	Reduced endocytic uptake at 37°C	Slow at 30°C *ts* at 37°C	Wendland *et al.*, 1996
*pan1-4 prk1*Δ	?	?	Suppression of *pan1-4 ts* growth	Zeng and Cai, 1999
*pan1-20 ent1*Δ	Similar to *pan1-20*	Similar to *pan1-20*	*ts* growth similar to *pan1-20*	This study
pan1-20 $ENT1^{AA}$[c]	Similar to *pan1-20*	Defective uptake less severe than *pan1-20*	*ts* growth is similar to *pan1-20*	This study
pan1-20 $ENT1^{EE}$[c]	Similar to *pan1-20*	Similar to *pan1-20*	*ts* growth defects enhanced	This study
*pan1-20 ent2*Δ	Similar to *pan1-20*	Partial suppression of endocytic defect	*ts* growth less severe than *pan1-20*	This study
pan1-20 $ENT1^{AA}$ ent2Δ	Similar to *pan1-20*	Similar to *pan1-20 ent2*Δ	Similar to *pan1-20 ent2*Δ	This study
pan1-20 $ENT1^{EE}$ *ent2*Δ	Similar to *pan1-20* $ENT1^{EE}$	Similar to *pan1-20* $ENT1^{EE}$	Similar to *pan1-20* $ENT1^{EE}$	This study

[a] No differences observed between wild-type cells and wild-type cells or *ent1*Δ cells overexpressing either $ENT1^{AA}$ or $ENT1^{EE}$.

[b] No differences observed between wild-type cells and wild-type cells overexpressing *ENT2*.

[c] No differences observed between wild-type or *ent2*Δ cells containing chromosomally integrated $ENT1^{AA}$ or $ENT1^{EE}$ and non-chromosomally integrated wild-type cells.

type Ent1p, integrated $Ent1p^{EE}$ is present at higher levels (approximately fourfold) (Figure 1B, lane 2). This may represent either elevated expression or increased stability of the $Ent1p^{EE}$ protein.

Next, *pan1–20 ent1* double-mutant strains were generated by mating integrated $ENT1^{AA}$ *ent2*Δ or integrated $ENT1^{EE}$ ent2Δ cells with *pan1–20* cells, followed by sporulation and dissection of the resultant meiotic recombinant haploid spores. In this way we were able to analyze *pan1* interactions with $ENT1^{AA}$ and $ENT1^{EE}$ in the presence and absence of *ENT2*. Growth and endocytic and actin defects of the strains were analyzed. The results are described below and summarized in Table 2.

Growth Defects

pan1–20 mutants exhibit poor growth on rich medium at 37°C. *pan1–20* $ENT1^{AA}$ cells showed temperature-sensitive growth defects similar to *pan1–20* on rich medium at 37°C. In contrast, we found that *pan1–20* $ENT1^{EE}$ cells grew even more poorly than *pan1–20* alone (Table 2). Interestingly, we found that *pan1–20* temperature sensitive growth was partially suppressed in a *pan1–20 ent2*Δ double mutant. *pan1–20* $ENT1^{AA}$ ent2Δ triple mutants grew similarly to *pan1–20 ent2*Δ cells, whereas *pan1–20* $ENT1^{EE}$ ent2Δ triple mutants grew almost as poorly as *pan1–20* $ENT1^{EE}$ double mutants, indicating that deleting *ENT2* cannot overcome the deleterious effects of combining *pan1–20* with $ENT1^{EE}$. We later isolated *pan1–20 ent1*Δ double-mutant cells and found that they exhibit similar *ts* growth at 37°C as *pan1–20* and *pan1–20* $ENT1^{AA}$ mutants (Table 2). The synergistic growth defects of *pan1–20* $ENT1^{EE}$ double mutants suggest that, consistent with *pan1–4 prk1*Δ data (Zeng and Cai, 1999), constitutively phosphorylated Ent1p may also be inhibitory to Pan1p function.

Endocytic Defects

Endocytic function was assessed with the use of FM 4–64 dye uptake experiments with the above strains. Cells were

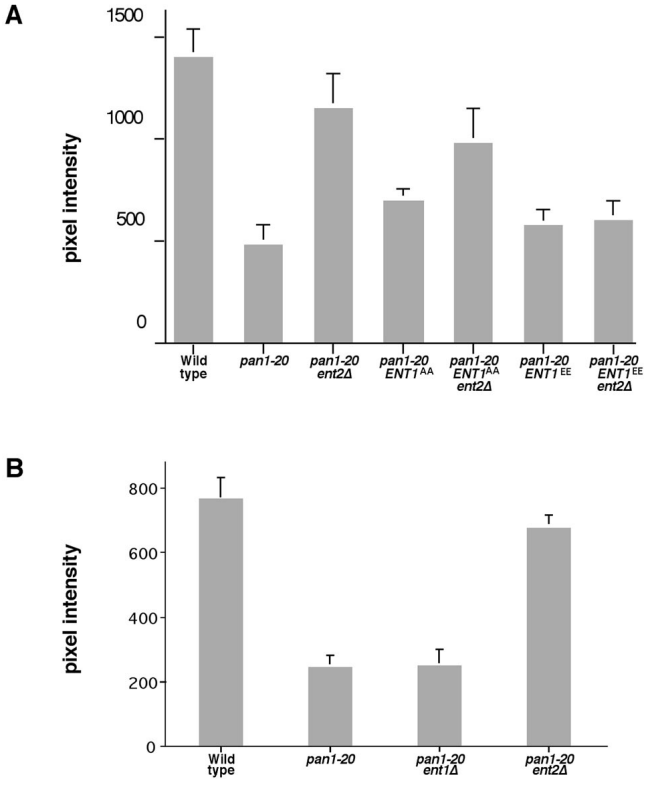

Figure 2. Effects of *ENT1*^{AA}, *ENT1*^{EE}, and *ent2*Δ on *pan1–20* growth and endocytic defects. Cells were grown to midlog phase in rich medium at 30°C, preshifted to 37°C for 30–45 min, and labeled with the lipophilic dye FM 4–64 at either 30 or 37°C for 15–20 min. After a 30–45 min chase period, cells were washed and observed with the use of fluorescence microscopy. (A) Pixel intensity values (35–50 cells per sample) refer to quantitation from a single focal plane of vacuolar membrane fluorescence after dye uptake and are as follows: wild-type, 1400 ± 130; *pan1–20*, 483 ± 90; *pan1–20 ent2*Δ, 1150 ± 170; *pan1–20 ENT1*^{AA}, 700 ± 60; *pan1–20 ent2*Δ *ENT1*^{AA}, 984 ± 160; *pan1–20 ENT1*^{EE}, 565 ± 90; *pan1–20 ent2*Δ *ENT1*^{EE}, 595 ± 100. (B) The FM 4–64 uptake assay at 37°C was performed as described above on wild-type, *pan1–20*, *pan1–20 ent1*Δ, and *pan1–20 ent2*Δ cells. Pixel intensities in this experiment were lower because of differences in labeling times and are as follows: wild-type, 765 ± 26; *pan1–20*, 244 ± 12; *pan1–20 ent1*Δ, 250 ± 17; and *pan1–20 ent2*Δ, 677 ± 12.

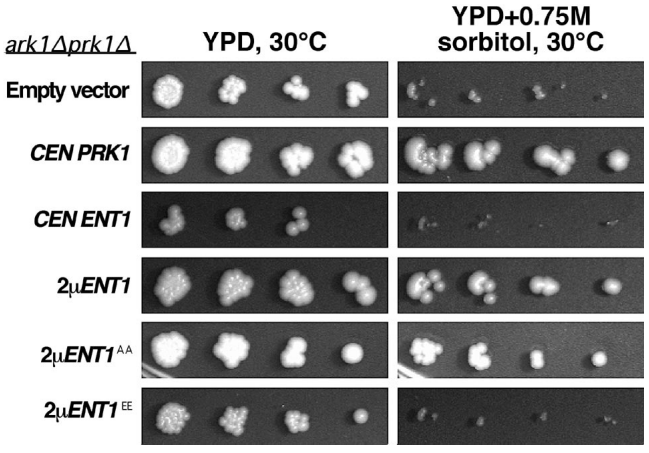

Figure 3. High copy *ENT1* and *ENT1*^{AA} can suppress *ark1*Δ *prk1*Δ sorbitol sensitivity. Cells transformed with empty vector, single copy (abbreviated, CEN)*PRK1* plasmid, and single or high copy (abbreviated, 2 μ) *ENT1*, *ENT1*^{AA}, and *ENT1*^{EE} were grown overnight in selective medium. Serial dilutions of each strain were spotted onto plates containing either rich medium (YPD, left panels) or sorbitol (YPD + 0.75 M sorbitol, right panels) and grown at 30°C for 3 d.

grown to midlog phase at 30°C and shifted to 37°C for 30–45 min. After the temperature shift, cells were labeled with the lipophilic FM 4–64 dye followed by a chase period. This dye associates with the outer leaflet of the plasma membrane and can be used to follow membranes as they travel through the endocytic pathway from the plasma membrane to the vacuolar membrane, in a time-, energy-, and temperature-dependent manner (Vida and Emr, 1995; Zheng *et al.*, 1998).

Figure 2A shows a graph quantitatively comparing FM 4–64 dye uptake in rich medium at 37°C in wild-type, *pan1–20*, *pan1–20 ENT1*^{AA}, *pan1–20 ENT1*^{EE}, and *pan1–20 ent2*Δ mutant cells as determined by pixel intensity values of vacuolar membrane fluorescence from a single focal plane. Vacuolar morphology was similar in all cases; however, intensity of labeling varied. *pan1–20 ENT1*^{AA} (700 ± 60) double-mutant cells internalized slightly more dye than *pan1–20* alone (485 ± 90), whereas *pan1–20 ENT1*^{EE} (565 ± 90) dye uptake was roughly similar to that of *pan1–20*. Consistent with improved growth at 37°C, internalization of FM 4–64 in *pan1–20 ent2*Δ (1150 ± 170) was restored to nearly wild-type levels (1400 ± 130), and the vacuoles were, on average, twice as bright as *pan1–20* cells. Also, as observed in the growth experiments, an *ent2*Δ mutation can partially rescue the *pan1–20* internalization defect in combination with *ENT1*^{AA} (984 ± 160) but not *ENT1*^{EE} (595 ± 100).

In separate experiments, when FM 4–64 internalization was compared between *pan1–20 ent1*Δ and *pan1–20 ent2*Δ mutants (Figure 2B), we found that, as with temperature sensitive growth, *ent1*Δ could not suppress the endocytic defects of *pan1–20* as compared with *ent2*Δ. These data provide a previously unobserved distinction between Ent1p and Ent2p function.

High Copy ENT1 and ENT1^{AA} *Can Suppress ark1*Δ *prk1*Δ *Defects*

Our biochemical data indicate that Prk1p alone is required for Ent1p and Ent2p threonine phosphorylation. Cope *et al.* (1999) found that *ark1*Δ and *prk1*Δ single deletion mutants behave similarly to wild-type cells, whereas *ark1*Δ *prk1*Δ double-deletion mutants exhibit poor growth and severe actin cytoskeleton defects. These data suggest that Ark1p and Prk1p may perform a redundant function or are components of an essential complex that requires the activity of at least one of the proteins. As a test of whether Ent1p and Ent2p might be down-stream targets of Ark1p/Prk1p function in vivo, we looked for genetic interactions between *ENT1* and *ENT2* and the *ark1*Δ *prk1*Δ mutants.

Sorbitol and Temperature Sensitivity Suppression

*ark1*Δ *prk1*Δ cells are sensitive to growth on sorbitol-containing medium at 30°C, as shown in the top panels of Figure 3. Serial dilutions of cells transformed with either empty vector or complemented with a single-copy *PRK1* plasmid were spotted onto rich medium ± sorbitol and grown at 30°C for 3 d. *PRK1* complemented cells grew well on both media, whereas the growth of empty vector-containing cells was severely reduced on sorbitol medium.

As shown in Figure 3, high copy *ENT1* was able to suppress the sorbitol sensitivity of *ark1*Δ *prk1*Δ cells. High copy $ENT1^{AA}$ suppressed sorbitol sensitivity comparably with high copy *ENT1*, whereas high copy $ENT1^{EE}$ did not suppress these growth defects, and in fact was deleterious. Temperature sensitivity is fully suppressed by *PRK1* and was also partially suppressed only by high copy *ENT1* or high copy $ENT1^{AA}$. Interestingly, high copy *ENT2* was unable to suppress either growth defect of double kinase mutant cells (our unpublished results). The yAP180 proteins share a similar domain organization with the Ent proteins, and each contains one copy of the L/IxxQxTG motif. Overexpression of either of the two yAP180 proteins was also unable to suppress the *ark1*Δ *prk1*Δ sorbitol-sensitive growth phenotype. These data demonstrate that *ENT1* is an in vivo target of Ark1p/Prk1p regulation and furthermore reveals a surprisingly specific property of Ent1p for suppression of *ark1*Δ *prk1*Δ phenotypes.

Endocytic Defect Suppression

Uptake of the fluorescent fluid-phase marker Lucifer yellow (LY) was used to monitor endocytosis from the medium to the vacuole. We found that *ark1*Δ *prk1*Δ cells exhibit defective endocytic uptake of LY, which, as with other defects, can be suppressed by single-copy *PRK1* (Figure 4Aa,b). As for sorbitol and temperature-sensitive growth, either high copy *ENT1* or $ENT1^{AA}$, but not $ENT1^{EE}$, was partially able to restore uptake of LY in the *ark1*Δ *prk1*Δ cells (Figure 4Ac–e). Interestingly, high copy $ENT1^{EE}$ expression not only failed to restore *ark1*Δ *prk1*Δ LY uptake, but the cells accumulated a number of peripheral patches of concentrated marker at the cell surface (Figure 4Ae). Similar peripheral patches accumulated to a lesser extent in *ark1*Δ *prk1*Δ cells alone (Figure 4Aa). Patches like these have also been observed in yeast treated with the F-actin stabilizing drug, jasplakinolide, which induces both actin and endocytic defects similar to *ark1*Δ *prk1*Δ cells (Ayscough, 2000). Experiments with the use of the lipophilic dye FM 4–64 to follow endocytosis of membranes revealed similar results.

Actin Cytoskeleton Defect Suppression

The actin cytoskeleton provides the structural basis for cell polarity in most eukaryotic cells. In *S. cerevisiae*, the actin patches at the cell cortex show a polarized distribution at the sites of cell growth (buds and sites of cytokinesis) that changes throughout the cell cycle (Kilmartin and Adams, 1984). Cope *et al.* (1999) found that the filamentous actin of *ark1*Δ *prk1*Δ mutants accumulates in a few large clumps and that cortical actin patches are smaller than normal and no longer concentrated at sites of budding, as shown in Figure 4Ba. These actin defects can be fully suppressed by introducing a single functional copy of either *ARK1* or *PRK1*

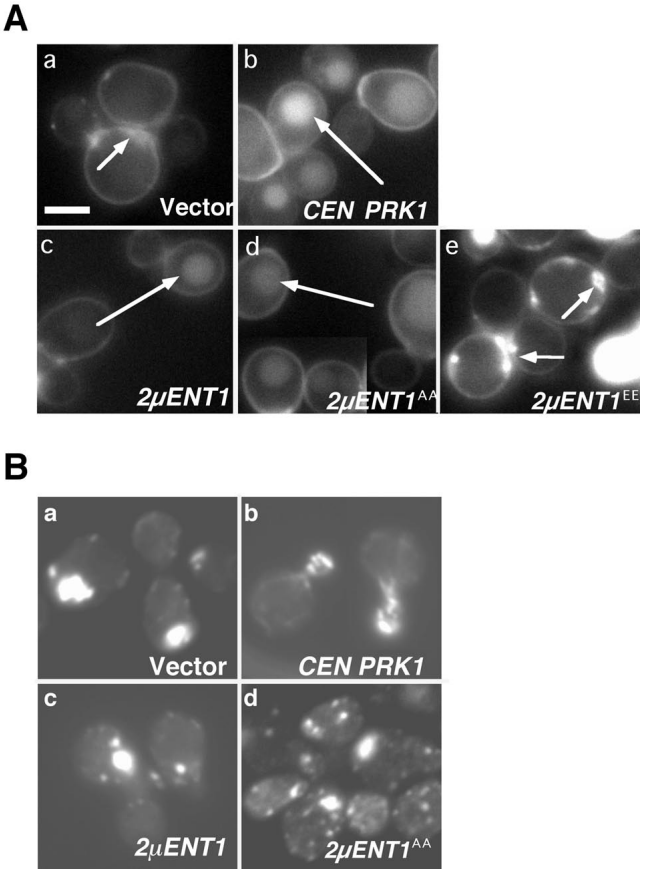

Figure 4. Overexpressing *ENT1* and $ENT1^{AA}$ but not $ENT1^{EE}$ partially suppresses the endocytosis and actin defects in *ark1*Δ *prk1*Δ mutant cells. (A) The fluorescent fluid-phase marker LY was used to monitor endocytosis from the medium to the vacuole interior, in cells transformed with (a) empty vector, (b) single copy *PRK1*, (c) 2 μ *ENT1*, (d) 2μ $ENT1^{AA}$, and (e) 2μ $ENT1^{EE}$. Vacuoles, long arrows; peripheral patches, short arrows. Bar, 2 μm. (B) Cells were grown overnight in selective media at 30°C and fixed, and filamentous actin was labeled with the use of Texas Red-conjugated phalloidin. Panel a corresponds to *ark1*Δ *prk1*Δ cells with empty vector, panels b–d correspond to *ark1*Δ *prk1*Δ with single copy *PRK1*, high copy *ENT1*, and $ENT1^{AA}$, respectively.

(Figure 4Bb) (see also Cope *et al.*,1999). As seen with the sorbitol sensitivity and LY uptake, high copy $ENT1^{AA}$ was able to partially suppress the accumulation of actin clumps in *ark1*Δ *prk1*Δ cells (Figure 4Bd). Although most of the filamentous actin remains in the characteristic large clumps, an increased number of smaller, peripherally localized patches was observed in *ark1*Δ *prk1*Δ mutants expressing $ENT1^{AA}$. Interestingly, partial suppression of actin clump accumulation occurred to a significantly lesser extent with high copy *ENT1* (Figure 4Bc). Consistent with our other suppression studies, neither $ENT1^{EE}$ nor *ENT2* overexpression suppressed these actin localization defects. Together, the findings that *ent2*Δ but not *ent1*Δ rescued *pan1–20* defects and the observed differences in the genetic interactions among *ENT1*, *ENT2*, and the *ark1*Δ *prk1*Δ double mutants all support the conclusion that *ENT1* and *ENT2* are at least

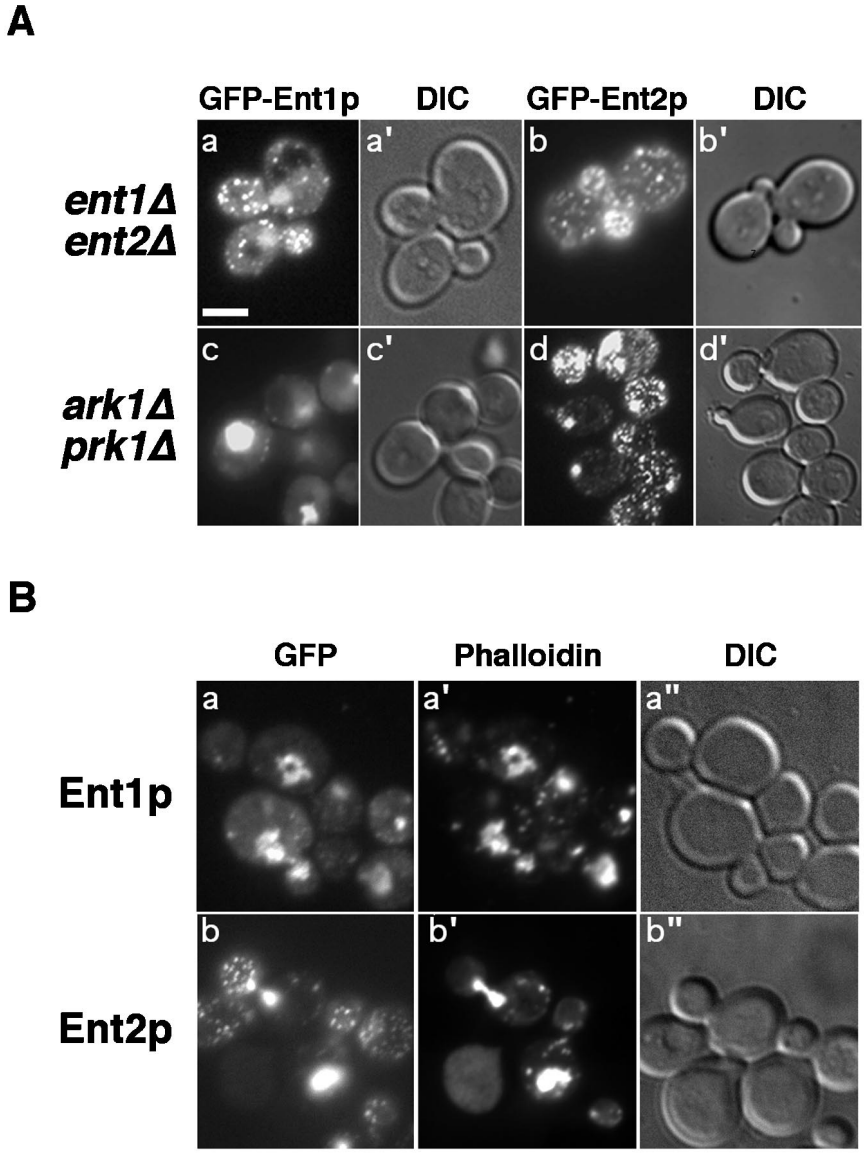

Figure 5. Ent1p-GFP and Ent2p-GFP colocalize with actin clumps in *ark1*Δ*prk1*Δ mutant cells. (A) GFP localization of Ent1p and Ent2p in *ent1*Δ *ent2*Δ and *ark1*Δ *prk1*Δ cells. *ent1*Δ *ent2*Δ and *ark1*Δ *prk1*Δ cells transformed with high copy plasmids encoding GFP-tagged Ent1p (GFP-Ent1p) or GFP-tagged Ent2p (GFP-Ent2p) were grown overnight in selective media and observed by fluorescence microscopy. Bar, 4 μm. (B) Ent1p-GFP and Ent2p-GFP colocalization with phalloidin-labeled *ark1*Δ *prk1*Δ cells. *ark1*Δ *prk1*Δ cells transformed with GFP-Ent1p or GFP-Ent2p were grown to midlog phase, harvested, and resuspended in permeabilization buffer containing Texas Red-conjugated phalloidin without fixation. Cells were incubated at room temperature for 10 min, followed by 20 min on ice, then observed by fluorescence microscopy.

partially functionally distinct. Furthermore, it appears that Prk1p phosphorylation either inhibits Ent1p function or negatively regulates the activity of a Pan1p/Ent1p complex.

GFP-Ent1p Localizes to Actin Clumps in ark1Δ prk1Δ Cells

Filamentous actin clumps of *ark1*Δ *prk1*Δ cells contain Sac6p, cofilin, Sla2p, and Abp1p, all of which are known cortical actin patch constituents (Cope *et al.*, 1999). We next determined the localization of GFP-Ent1p and GFP-Ent2p in these mutants. GFP-Ent1p and GFP-Ent2p are each stable proteins that fully rescue lethality of *ent1*Δ *ent2*Δ cells. In *ent1*Δ *ent2*Δ cells, GFP-Ent1p localizes to peripheral and internal punctate structures (Figure 5Aa) in a pattern suggestive of its association with plasma membrane-associated patches and/or early endosomes, and consistent with its partial colocalization with cortical actin patches (Wendland *et al.*, 1999). Localization patterns were identical for both single and high copy plasmid. It should be noted that expression levels of high copy GFP-Ent1p driven by the CPY promoter were not as elevated as with high copy *ENT1* driven by its endogenous promoter. GFP-Ent2p also localizes to peripheral and internal punctate structures in both wild-type and *ent1*Δ *ent2*Δ cells; however, the peripheral structures are finer and more diffuse (Figure 5Ab). In *ark1*Δ *prk1*Δ cells, GFP-Ent1p and to a lesser extent, GFP-Ent2p, accumulated in large clumps that were reminiscent of the aberrant filamentous actin structures observed previously in these mutants (Figure 5Ac,d).

To determine whether GFP-Ent1p or GFP-Ent2p colocalizes with filamentous actin, wild-type and *ark1*Δ *prk1*Δ mutant cells expressing GFP-Ent1p and GFP-Ent2p were la-

beled with Texas Red-conjugated phalloidin, an F-actin–binding toxin that prevents F-actin depolymerization. Interestingly, fixation methods used for phalloidin labeling consistently caused dispersal of these GFP fusion proteins. Instead, we found that phalloidin stabilization of actin filaments in saponin-permeabilized cells without previous fixation was able to preserve GFP-Ent1p and GFP-Ent2p localization. In these experiments, GFP-Ent1p colocalized exactly with both large actin clumps and small peripheral actin patches in *ark1*Δ *prk1*Δ mutants (Figure 5B, top panels). In contrast, although a portion of GFP-Ent2p also localized to these clumps, the majority of GFP-Ent2p remained highly dispersed in small phalloidin-negative patches at the cell periphery (Figure 5B, bottom panels). Similar to GFP-Ent2p, GFP-Pan1p and the GFP-yAP180 proteins also did not localize exclusively to the large actin clumps in *ark1*Δ *prk1*Δ cells (our unpublished results). This difference in localization between Ent1p and Ent2p provides further evidence to support a functional distinction between the two proteins.

DISCUSSION

The ARK kinases Ark1p and Prk1p have been implicated in regulation of the actin cytoskeleton because of their localization at cortical actin patches and their requirement for normal actin organization. Genetic interactions with and phosphorylation of proteins implicated in endocytosis suggested that the ARK kinases might also be important for regulating endocytosis; however, this had not been tested directly. In this study, we have found that the ARK kinases are also necessary for efficient fluid phase endocytosis. This indicated that the targets of these kinases should not only be proteins that control actin cytoskeleton structure, but also might be endocytic proteins. Indeed, we found that the yeast epsin homologues Ent1p and Ent2p are phosphorylated on threonine residues in a *PRK1*-dependent manner, and that the phosphorylation status of Ent1p appears to modulate its ability to support endocytosis. Finally, this study has also revealed interesting functional distinctions between the highly homologous Ent1p and Ent2p proteins.

Threonine Phosphorylation of the Yeast Epsins Ent1p and Ent2p Is Dependent on Prk1p

Pan1p was recently identified as an in vitro target for threonine phosphorylation by the serine/threonine kinase Prk1p on regions containing a total of 13 repeats of the consensus sequence LxxQxTG (Zeng and Cai, 1999). Yeast genome searches showed that Ent1p and Ent2p each contain two copies of an L/IxxQxTG sequence. We have demonstrated that these are the only two sites required for threonine phosphorylation in Ent1p, and that Prk1p is required for this modification. Interestingly, there are several other proteins predicted by the yeast genome sequence that contain multiple copies of this consensus sequence or slight variations of it, including the actin-associated protein, Sla1p, and the clathrin-associated factor, Scd5p (*S. cerevisiae* Genome Database Pattern Match [Holtzman *et al.*, 1993; Nelson *et al.*, 1996]). It will be of great interest to determine whether these proteins are also modified and regulated by Prk1p. Additionally, future identification of targets of the related Ark1p kinase should also reveal important regulators of endocytosis.

Ent1p and Ent2p May Perform Distinct Roles in Endocytic and Actin Functions

Previous data have shown that at least one functional copy of either an Ent1p or an Ent2p ENTH domain is required for yeast cell viability, which suggested that the two proteins perform redundant functions (Wendland *et al.*, 1999). Our new findings reported here, however, indicate that in addition to their redundant functions, distinct functional roles are performed by Ent1p and Ent2p, possibly independent of their ENTH domains. For instance, converting the two Prk1p consensus site threonines in Ent1p to either alanine or glutamic acid residues resulted in significantly reduced detection by phosphothreonine antiserum, whereas analogous mutations in Ent2p did not. In contrast, total phosphothreonine levels appear to be Prk1p dependent for both Ent1p and Ent2p, as seen in *prk1*Δ cell extracts. These data suggest that other potential Prk1p-dependent threonine phosphorylation sites are present in Ent2p. This may indicate that either Prk1p can phosphorylate a broader range of consensus sites in Ent2p (and possibly other proteins) or that Ent2p threonines are phosphorylated by other kinases downstream of Prk1p.

Distinctions between Ent1p and Ent2p were also observed in phenotype suppression studies in *pan1–20* and *ark1*Δ *prk1*Δ mutant cells. High copy *ENT1* partially suppressed *ark1*Δ *prk1*Δ mutant defects, whereas high copy *ENT2* did not. Additionally, GFP-Ent1p mislocalized to the actin clumps of *ark1*Δ *prk1*Δ cells, similarly to other cortical actin patch constituents such as Sla2p, cofilin, and Abp1p, whereas only a portion of GFP-Ent2p was similarly mislocalized. Finally, combining *ent2*Δ with *pan1–20* suppressed growth and endocytic defects of the *pan1–20* mutant, whereas a *pan1–20 ent1*Δ double mutant behaved essentially identically to *pan1–20* cells. This observation suggested that Ent2p interactions with Pan1p may inhibit Pan1p-dependent endocytic processes. Consistent with this idea, overexpressing *ENT2*, but not *ENT1*, enhanced *pan1–20* growth defects (our unpublished results). The role of Ent2p in Ark1p/Prk1p-regulated events is not yet clear. Because GFP-Ent2p localization is relatively resistant to loss of Ark1p/Prk1p activity, Ent2p may be less sensitive to ARK kinase regulation, regulated by additional enzymes, or have a unique set of binding partners relative to Ent1p. These differences might also be related to the apparent inhibition of Pan1p by Ent2p.

Interestingly, mammalian cells also contain two genes encoding highly related epsins, epsin1 and epsin2/Ibp2 (Hussain *et al.*, 1999; Rosenthal *et al.*, 1999). Epsin1 is phosphorylated by the mitotic kinase cdc2, whereas epsin2 is not (Stukenberg *et al.*, 1997; Chen *et al.*, 1998; Rosenthal *et al.*, 1999). Thus, like the yeast epsins, the mammalian epsins may also be differentially regulated to perform distinct functions.

Ent1p Function in Endocytosis May Be Negatively Regulated by Prk1p Phosphorylation

Zeng and Cai (1999) found that *prk1*Δ suppresses the growth and actin defects of the *pan1–4* mutant, and that when in a complex with End3p, Pan1p is unavailable for in vitro Prk1p phosphorylation. Although the functional significance of a Pan1p/End3p interaction remains to be determined, these

data suggest that Prk1p phosphorylation inhibits Pan1p activity. Consistent with this, our data indicate that Ent1p activity is inhibited by Prk1p phosphorylation. Importantly, our data also suggest that Ark1p/Prk1p activity is necessary to regulate endocytosis and that Ent1p is one of the critical in vivo targets of these kinases.

We were unable to detect significant effects of overexpressing the constitutively dephosphorylated mimic, *ENT1^{AA}*, or the constitutively phosphorylated mimic, *ENT1^{EE}*, in wild-type cells, and found only mild defects in *ent1*Δ *ent2*Δ cells expressing *ENT1^{EE}* either chromosomally or from a high copy plasmid. Instead, the effects of *ENT1^{AA}* or *ENT1^{EE}* were most apparent when combined with another mutation such as *ark1*Δ *prk1*Δ or *pan1–20*. We found that *ENT1^{EE}* but not *ENT1^{AA}* increased the growth defects of *pan1–20* cells. Although *ENT1^{EE}* did not exacerbate *pan1–20* endocytic defects, it prohibited *ent2*Δ suppression of these defects. Taken together, these data suggest that Prk1p-mediated phosphorylation of Ent1p regulates Pan1p activity, possibly through modulating and EH/Asn-ProPhe interaction. Additionally, Ent2p may antagonize Ent1p or Pan1p; future experiments examining physical associations between these proteins in the presence or absence of kinases should shed light on this question. Previous precedence for phosphorylation of endocytic machinery having inhibitory consequences can be found in the example of the dephosphins (e.g., Eps15 and epsin), which are phosphorylated at rest and are coordinately dephosphorylated during stimulation of the nerve terminal to promote recycling of synaptic vesicle membranes (Chen *et al.*, 1999).

In this study, we also report that, in addition to their growth and severe actin defects, *ark1*Δ *prk1*Δ mutants are also defective in endocytosis. We found that high copy *ENT1^{EE}* increased the growth and endocytic defects of *ark1*Δ *prk1*Δ mutants, whereas high copy *ENT1^{AA}* partially suppressed these defects as well as the actin defects. Multiple kinase targets must be affected in *ark1*Δ *prk1*Δ cells; thus, it is somewhat surprising that the severe phenotypes of *ark1*Δ *prk1*Δ cells can be ameliorated by the overexpression of one of these targets, *ENT1*. Together, these data suggest that phosphorylation of Ent1p inhibits its endocytic function(s) and that its dephosphorylated form has a positive role in promoting endocytosis. The suppression of the *ark1*Δ *prk1*Δ phenotypes by high copy *ENT1^{AA}* might be due to Ent1p having a role in de novo formation of endocytic complexes. Alternatively, high copy *ENT1^{AA}* might promote partial dissolution of the F-actin cortical patch/endocytic aggregate to form separate subcomplexes, some of which are active for endocytosis. For neither scenario would high copy *ENT1^{EE}* be expected to have suppressing activity if the phosphorylated form is inhibited for function, as our data suggest.

It is intriguing that the ENTH domain of mammalian epsin was recently found to bind phospholipid phosphatidylinositol 4,5 bisphosphate, in part through a highly conserved lysine residue (Itoh *et al.*, 2001). This lysine residue is present in both Ent1p and Ent2p; thus, it is possible that yeast epsin ENTH domains also bind to phospholipid phosphatidylinositol 4,5 bisphosphate and/or other phosphate-containing molecules. Interestingly, we have found recently that combining *ENT1^{AA}* with the ENTH domain mutation of the *ent1–1* temperature-sensitive allele allows growth of *ent1*Δ *ent2*Δ cells at high temperature (our unpublished results). This suggests that Prk1p-dependent phosphorylation of Ent1p might also act through regulation of intramolecular interactions between the ENTH domain and the Prk1p phosphorylation sites of Ent1p.

Many interesting questions remain, including identifying additional targets of Prk1p Ark1p and Akl1p and determining the in vivo function and regulation of Pan1p/Ent1p/Ent2p complexes. Future studies aimed at dissecting the composition and activities of the various protein complexes that form and dissociate during the endocytic cycle should reveal important new steps for regulating the process of endocytosis in both yeast and more complex eukaryotes and may reveal novel connections between endocytic and actin machinery.

ACKNOWLEDGMENTS

We thank J. Michael McCaffery and Gerry Sexton of the Johns Hopkins University Integrated Imaging Center for help with microscopy. We thank Kyle Cunningham for critical reading of this manuscript and many helpful suggestions. We also acknowledge Rosa Alcazar for initial studies of Ent1p phosphorylation. We thank the members of the Wendland lab for helpful discussions, and especially thank Cathy Sciambi for excellent technical assistance. These studies were supported by National Institutes of Health (NIH) grants GM60979 to B.W. and GM50399 to D.D., an NIH Training Grant to H.W., and a Human Frontier Science Research Fellowship to M.J.T.V.C. B.W. is also supported as a Burroughs Wellcome Fund New Investigator in the Pharmacological Sciences and by a March of Dimes Basil O'Connor Scholar.

REFERENCES

Ayscough, K.R. (2000). Endocytosis and the development of cell polarity in yeast require a dynamic F-actin cytoskeleton. Curr. Biol. *10*, 1587–1590.

Benmerah, A., Poupon, V., Cerf-Bensussan, N., and Dautry-Varsat, A. (2000). Mapping of Eps15 domains involved in its targeting to clathrin-coated pits. J. Biol. Chem. *275*, 3288–3295.

Carbone, R., Fre, S., Iannolo, G., Belleudi, F., Mancini, P., Pelicci, P.G., Torrisi, M.R., and Di Fiore, P.P. (1997). eps15 and eps15R are essential components of the endocytic pathway. Cancer Res. *57*, 5498–5504.

Chen, H., Fre, S., Slepnev, V.I., Capua, M.R., Takei, K., Butler, M.H., Di Fiore, P.P., and De Camilli, P. (1998). Epsin is an EH-domain-binding protein implicated in clathrin-mediated endocytosis. Nature *394*, 793–797.

Chen, H., Slepnev, V.I., Di Fiore, P.P., and De Camilli, P. (1999). The interaction of epsin and Eps15 with the clathrin adaptor AP-2 is inhibited by mitotic phosphorylation and enhanced by stimulation-dependent dephosphorylation in nerve terminals. J. Biol. Chem. *274*, 3257–3260.

Cope, M.J., Yang, S., Shang, C., and Drubin, D.G. (1999). Novel protein kinases Ark1p and Prk1p associate with and regulate the cortical actin cytoskeleton in budding yeast. J. Cell Biol. *144*, 1203–1218.

Cowles, C.R., Payne, G.S., and Emr, S.D. (1997). The AP-3 adaptor complex is essential for cargo-selective transport to the yeast vacuole. Cell *91*, 109–118.

de Beer, T., Carter, R.E., Lobel-Rice, K.E., Sorkin, A., and Overduin, M. (1998). Structure and Asn-Pro-Phe binding pocket of the Eps15 homology domain. Science *281*, 1357–1360.

de Beer, T., Hoofnagle, A.N., Enmon, J.L., Bowers, R.C., Yamabhai, M., Kay, B.K., and Overduin, M. (2000). Molecular mechanism of NPF recognition by EH domains. Nat. Struct. Biol. *7*, 1018–1022.

Holtzman, D.A., Yang, S., and Drubin, D.G. (1993). Synthetic-lethal interactions identify two novel genes, SLA1 and SLA2, that control membrane cytoskeleton assembly in *Saccharomyces cerevisiae*. J. Cell Biol. *122*, 635–644.

Hussain, N.K., Yamabhai, M., Ramjaun, A.R., Guy, A.M., Baranes, D., O'Bryan, J.P., Der, C.J., Kay, B.K., and McPherson, P.S. (1999). Splice variants of intersectin are components of the endocytic machinery in neurons and nonneuronal cells. J. Biol. Chem. *274*, 15671–15677.

Hyman, J., Chen, H., Di Fiore, P.P., De Camilli, P., and Brunger, A.T. (2000). Epsin 1 undergoes nucleocytosolic shuttling and its eps15 interactor NH(2)-terminal homology (ENTH) domain, structurally similar to Armadillo and HEAT repeats, interacts with the transcription factor promyelocytic leukemia Zn(2)+ finger protein (PLZF). J. Cell Biol. *149*, 537–546.

Itoh, T., Koshiba, S., Kigawa, T., Kikuchi, A., Yokoyama, S., and Takenawa, T. (2001). Role of the ENTH domain in phosphatidylinositol-4,5-bisphosphate binding and endocytosis. Science *291*, 1047–1051.

Kay, B.K., Yamabhai, M., Wendland, B., and Emr, S.D. (1999). Identification of a novel domain shared by putative components of the endocytic and cytoskeletal machinery. Protein Sci. *8*, 435–438.

Kilmartin, J.V., and Adams, A.E. (1984). Structural rearrangements of tubulin and actin during the cell cycle of the yeast *Saccharomyces*. J. Cell Biol. *98*, 922–933.

Mulholland, J., Konopka, J., Singer-Kruger, B., Zerial, M., and Botstein, D. (1999). Visualization of receptor-mediated endocytosis in yeast. Mol. Biol. Cell *10*, 799–817.

Nelson, K.K., Holmer, M., and Lemmon, S.K. (1996). SCD5, a suppressor of clathrin deficiency, encodes a novel protein with a late secretory function in yeast. Mol. Biol. Cell *7*, 245–260.

Qualmann, B., Kessels, M.M., and Kelly, R.B. (2000). Molecular links between endocytosis and the actin cytoskeleton. J. Cell Biol. *150*, F111–116.

Rosenthal, J.A., Chen, H., Slepnev, V.I., Pellegrini, L., Salcini, A.E., Di Fiore, P.P., and De Camilli, P. (1999). The epsins define a family of proteins that interact with components of the clathrin coat and contain a new protein module. J. Biol. Chem. *274*, 33959–33965.

Salcini, A.E., Chen, H., Iannolo, G., De Camilli, P., and Di Fiore, P.P. (1999). Epidermal growth factor pathway substrate 15, Eps15. Int. J. Biochem. Cell Biol. *31*, 805–809.

Schmid, S.L. (1997). Clathrin-coated vesicle formation and protein sorting: an integrated process. Annu. Rev. Biochem. *66*, 511–548.

Slepnev, V.I., Ochoa, G.C., Butler, M.H., Grabs, D., and Camilli, P.D. (1998). Role of phosphorylation in regulation of the assembly of endocytic coat complexes. Science *281*, 821–824.

Stukenberg, P.T., Lustig, K.D., McGarry, T.J., King, R.W., Kuang, J., and Kirschner, M.W. (1997). Systematic identification of mitotic phosphoproteins. Curr. Biol. *7*, 338–348.

Tang, H.Y., and Cai, M. (1996). The EH-domain-containing protein Pan1 is required for normal organization of the actin cytoskeleton in *Saccharomyces cerevisiae*. Mol. Cell. Biol. *16*, 4897–4914.

Tang, H.Y., Munn, A., and Cai, M. (1997). EH domain proteins Pan1p and End3p are components of a complex that plays a dual role in organization of the cortical actin cytoskeleton and endocytosis in *Saccharomyces cerevisiae*. Mol. Cell. Biol. *17*, 4294–4304.

Thiagalingam, S., Kinzler, K.W., and Vogelstein, B. (1995). PAK1, a gene that can regulate p53 activity in yeast. Proc. Natl. Acad. Sci. USA *92*, 6062–6066.

Vida, T.A., and Emr, S.D. (1995). A new vital stain for visualizing vacuolar membrane dynamics and endocytosis in yeast. J. Cell Biol. *128*, 779–792.

Wendland, B., and Emr, S.D. (1998). Pan1p, yeast eps15, functions as a multivalent adaptor that coordinates protein-protein interactions essential for endocytosis. J. Cell Biol. *141*, 71–84.

Wendland, B., McCaffery, J.M., Xiao, Q., and Emr, S.D. (1996). A novel fluorescence-activated cell sorter-based screen for yeast endocytosis mutants identifies a yeast homologue of mammalian eps15. J. Cell Biol. *135*, 1485–1500.

Wendland, B., Steece, K.E., and Emr, S.D. (1999). Yeast epsins contain an essential N-terminal ENTH domain, bind clathrin and are required for endocytosis. EMBO J. *18*, 4383–4393.

Wong, W.T., Schumacher, C., Salcini, A.E., Romano, A., Castagnino, P., Pelicci, P.G., and Di Fiore, P. (1995). A protein-binding domain, EH, identified in the receptor tyrosine kinase substrate Eps15 and conserved in evolution. Proc. Natl. Acad. Sci. USA *92*, 9530–9534.

Zeng, G., and Cai, M. (1999). Regulation of the actin cytoskeleton organization in yeast by a novel serine/threonine kinase Prk1p. J. Cell Biol. *144*, 71–82.

Zheng, B., Wu, J.N., Schober, W., Lewis, D.E., and Vida, T. (1998). Isolation of yeast mutants defective for localization of vacuolar vital dyes. Proc. Natl. Acad. Sci. USA *95*, 11721–11726.

Zoladek, T., Vaduva, G., Hunter, L.A., Boguta, M., Go, B.D., Martin, N.C., and Hopper, A.K. (1995). Mutations altering the mitochondrial-cytoplasmic distribution of Mod5p implicate the actin cytoskeleton and mRNA 3′ ends and/or protein synthesis in mitochondrial delivery. Mol. Cell. Biol. *15*, 6884–6894.